

# Journal of Visualized Experiments

## In vitro preparation of actively maturing bovine articular cartilage explants for X-ray phase contrast imaging --Manuscript Draft--

Article Type:	Invited Methods Article - JoVE Produced Video
Manuscript Number:	JoVE61607R2
Full Title:	In vitro preparation of actively maturing bovine articular cartilage explants for X-ray phase contrast imaging
Section/Category:	JoVE Bioengineering
Keywords:	Articular Cartilage; Maturation; Synchrotron Radiation; X-ray Phase Contrast Imaging,
Corresponding Author:	Emmanuel Brun Inserm Grenoble, Grenoble FRANCE
Corresponding Author's Institution:	Inserm
Corresponding Author E-Mail:	emmanuel.brun@inserm.fr
Order of Authors:	Caroline Bissardon Yadan Zhang Hélène Rougé Labriet Sébastien berujon Laurent Charlet Ilyas Khan Emmanuel Brun Sylvain Bohic
Additional Information:	
Question	Response
Please indicate whether this article will be Standard Access or Open Access.	Standard Access (US\$2,400)
Please indicate the <b>city, state/province, and country</b> where this article will be <b>filmed</b> . Please do not use abbreviations.	Grenoble France

## In Vitro Preparation of Actively Maturing Bovine Articular Cartilage Explants for X-Ray Phase Contrast Imaging

Caroline Bissardon<sup>1,2,3</sup>, Yadan Zhang<sup>2</sup>, H  l  ne Roug   Labriet<sup>1,4</sup>, S  bastien B  rujon<sup>5</sup>, Laurent Charlet<sup>3</sup>, Ilyas M. Khan<sup>2</sup>, Emmanuel Brun<sup>1</sup>, Sylvain Bohic<sup>1</sup>

<sup>5</sup>ESRF, European Synchrotron Radiation Facility, CS, Grenoble Cedex 9, France

Emmanuel Brun (emmanuel.brun@inserm.fr)

Sylvain Bohic (bohic@esrf.fr)

articular cartilage, maturation, synchrotron radiation, X-ray phase contrast imaging, propagation-based imaging, regenerative medicine

This protocol describes the preparation of in vitro bovine articular cartilage for imaging in high resolution with X-rays. These explants actively undergo postnatal maturation. We describe here the necessary steps from the biopsy to data analysis of 3D X-ray phase contrast imaging, passing through explant culture, tissue fixation and synchrotron preparation.

Understanding the mechanisms that underpin post-natal maturation of articular cartilage is of crucial importance for designing the next generation of tissue engineering strategies and potentially repairing diseased or damaged cartilage. In general, postnatal maturation of the articular cartilage, which is a wholesale change in collagen structure and function of the tissue to accommodate growth of the organism, occurs over a timescale ranging from months to years. Conversely dissolution of the structural organization of the cartilage that also occurs over long timescales is the hallmark of tissue degeneration. Our ability to study these biological processes

in detail have been enhanced by the findings that growth factors can induce precocious in vitro maturation of immature articular cartilage. The developmental and disease related changes that occur in the joint involve bone and cartilage and an ability to co-image these tissues would significantly increase our understanding of their intertwined roles.

The simultaneous visualization of soft tissue, cartilage and bone changes is nowadays a challenge to overcome for conventional preclinical imaging modalities used for the joint disease follow-up. Three-dimensional X-ray Phase-Contrast Imaging methods (PCI) have been under perpetual developments for 20 years due to high performance for imaging low density objects and their ability to provide additional information compared to conventional X-ray imaging.

In this protocol we detail the procedure used in our experiments from biopsy of the cartilage, generation of in vitro matured cartilage to data analysis of image collected using X-ray phase contrast imaging.

## **INTRODUCTION:**

Immature articular cartilage is an adequate support to initiate morphological, structural and biomolecular changes<sup>1</sup> in order to obtain an adult joint-specific function. The principal change is reorganization of collagen fibrils from one displaying a parallel orientation with respect to the surface in immature cartilage to one where fibrils deeper in the tissue are perpendicular in mature cartilage. Pseudo-stratification of adult cartilage is evident through the reorganization of resident chondrocytes along the direction of collagen fibril orientation with cells at the surface disc-like and parallel to the surface and in the deeper zones cells becoming progressively larger and organized in columns. Post-natal maturation is known to occur over many months and is essentially completed at the end of puberty, the long timescale was thought to make studying this important developmental transition at best difficult or technically impossible to study in detail<sup>2</sup>. Some advances into the solution to this problem have been made through the finding that fibroblast growth factor-2 and transforming growth factor- $\beta$ 1 together are able to induce important physiological and morphological changes that replicate articular cartilage maturation<sup>2,3</sup> (**Figure 1**). Growth factor-induced in vitro maturation occurs within three weeks and does not require any biomechanical input. After culture, collagen type II expression is significantly reduced and the ratio of mature trivalent to immature divalent collagen crosslinks increases as is seen in maturing cartilage. Also, the organization of the extracellular matrix and collagen fibrils is closer to that seen in mature cartilage though this facet of transition is not complete. Biochemically, the composition of growth factor-treated cartilage is mimicking an adult articular cartilage<sup>3</sup>.

The model used in the article is based on an in vitro culture of 4- or 6-mm diameter explants that were excised under sterile conditions from the lateral aspect of the metacarpophalangeal joint medial condyle from immature male (7 days-old) bovine steers. A thin layer of calcified cartilage and subchondral bone was kept on the basal aspect of each explant. The articular cartilage were cultured in a classical serum-free medium Dulbecco's modified Eagles medium (high glucose 4.5 g/L) in which insulin-transferrin-selenium (ITS), 10 mM HEPES buffer pH 7.4, ascorbic acid and 50  $\mu$ g/mL gentamicin were added. This culture medium is supplemented with 100 ng/mL

fibroblast growth factor 2 (FGF-2) and 10 ng/mL transforming growth factor  $\beta$ 1 (TGF- $\beta$ 1) that are replenished every third day with media changes<sup>2</sup>. Highly accelerated cartilage maturation is induced by combining growth factors. These changes occur within 21 days. Growth factor stimulation additionally induces apoptosis and resorption from the basal aspect and cellular proliferation in surface chondrocytes<sup>3</sup>. The culture medium composition is described in **Table 1**. Following the model developed by Khan et al. 2011<sup>2</sup>, articular cartilage explants are cultured with TGF- $\beta$ 1 at a concentration of 10 ng/ $\mu$ L and FGF2 at 100 ng/ $\mu$ L concentration (stock concentrations 10  $\mu$ g/mL and 100  $\mu$ g/mL dissolved in phosphate buffered saline/0.1% BSA). 1  $\mu$ L of each growth factor is used per 1 mL of the medium. DMEM-F12 with L- glutamine and high glucose is an artificial medium which, once supplemented with insulin, transferrin and selenium (ITS), ascorbic acid, gentamicin and HEPES provides a complete medium supplementation with all the physiological growth requirements specific to the different cell lines and explants cultures. DMEM-F12 is composed of several diverse inorganic salts (i.e., NaCl, KCl, CaCl<sub>2</sub>, MgCl<sub>2</sub>, NaH<sub>2</sub>PO<sub>4</sub>), glucose, amino acids (nitrogen sources), vitamins, co-factors and water. Those salts provide adequate energetic inputs to sustain the cellular survival and normal growth in culture. The mineral ions contribute to maintaining the osmolarity close to the natural physiological environment. The higher concentration of glucose (4.5 g/L) is used as chondrocytes respire primarily through glycolysis. F12 medium supplementation is used because it offers number of sources of sulfate, CuSO<sub>4</sub>, FeSO<sub>4</sub>, ZnSO<sub>4</sub> and MgSO<sub>4</sub> required for sulfated glycosaminoglycan synthesis. As checked by colored indicators (here phenol red) and CO<sub>2</sub>/HCO<sub>3</sub><sup>-</sup> buffer combined with phosphates, the pH remains constant at a value close to 7.4. The major respiratory pathway used by chondrocytes is glycolysis where lactic acid is the end product which causes an increase in pH, therefore, in the absence of biomechanical forces that would help to remove locally produced lactic acid, HEPES acts to maintain a buffered environment for physiological processes. Gentamicin is an aminoglycoside antibiotic controls external bacterial contamination through inhibition of growth. Ascorbic acid is used as medium complement for its anti-oxidant action<sup>4</sup>. Ascorbic acid is a co-factor for enzymes, prolyl hydroxylases, that function to hydroxylate proline residues in collagen stabilizing its triple helical structure. The transferrin usually serves as extracellular antioxidant (toxicity and ROS reductions)<sup>5,6</sup>. It is also added to the culture medium for its ability to provide and facilitate extracellular iron storage and transport in cell culture. Transferrin binds iron so tightly under physiological conditions that virtually no free iron exists to catalyze the production of free radicals<sup>7</sup>. The insulin hormone signaling from its bound receptor increases the absorption of several elements such as glucose, amino acids. It is also involved in several processes such as intracellular transport, lipogenesis, protein, and nucleic acid syntheses. Insulin has a growth-promoting effect. Selenium is present additionally in the composite solution “insulin-transferrin-selenium”, as sodium selenite. It is mainly used as a cofactor for (seleno-) proteins such glutathione peroxidase (GPX), as supplementary antioxidant agent in the culture. In in vitro articular chondrocytes, ITS seems to enhance cellular proliferation and phenotype preservation by inhibiting the gene expression related to cellular dedifferentiation and hypertrophic differentiation<sup>8</sup>. Growth factors like fibroblast growth factor-2 and transforming growth factor- $\beta$ 1 are added to the culture medium. They are used to induce and regulate cell differentiation, growth, healing, and development<sup>2,3</sup>. FGF-2 and TGF- $\beta$ 1 in combination also potently promote cellular proliferation in cultured cells and tissues<sup>9</sup>.

This in vitro maturation model of articular cartilage is useful for three main reasons. First, the accelerated developmental phase transition in this model allows us to study imperceptible changes that occur over many months in in vivo models such as the elevated expression of lysyl oxidase-L1 during maturation<sup>10</sup>. Secondly, tissue engineering of articular cartilage suffers from the fact that cartilage with an isotropic morphology and structure is produced which is functionally deficient when transplanted into joints to repair focal defects. Understanding how to induce maturational changes will accelerate the development of fully functional implantable devices. Thirdly and pertinent to this study, there are degenerative joint conditions such as Kashin-Beck disease occurring during childhood that lead to severe joint deformities in adulthood. This particular disease is strongly associated to geographic areas (China) with endemic deficiencies in selenium and iodine potentially affecting tens of millions of inhabitants<sup>11–13</sup>. Examination of skeletal defects in Kashin-Beck disease show that it occurs peripubertally, implicating perturbation of skeletal maturational processes. Therefore, to further understand the role of selenium in articular cartilage (AC) a robust model for cartilage growth and development is required. An in vitro growth factor-induced model of maturation provides a useful starting point for studies on the growth and metabolism of articular cartilage during maturation in presence or absence of selenium ions<sup>14–16</sup>. Our knowledge of the effects of selenium (Se) deficiency on complex and inter-related biological processes remains very poor. The main problem lies in the fact that selenium remains an element to study due to its restrictive action range (required concentration between 40 and 400 µg/kg<sup>17</sup>) and the very low concentration involved. The accelerated maturation model using immature bovine cartilage offers an unprecedented ability to look at biological changes that occur during an important phase of development. The Se-concentration in organisms is tightly controlled, and this model is a starting point to develop imaging techniques allowing its precise tracking during maturation. These techniques could then be a powerful tool to study strategies to prevent AC degradation and potentially to develop the basis of novel regenerative medicine-based therapies.

Simultaneous visualization of soft tissue, cartilage and bone changes is a major challenge in conventional preclinical imaging modalities. This would be indeed an important help for joint disease follow-up<sup>18,19</sup>. As an example, conventional X-ray micro Computed Tomography (µCT) presents poor performances for soft tissue that limit its use to the depiction of bone defects, osteophytes, and indirect visualization of cartilage. Magnetic Resonance Imaging (MRI), on the other hand, is conventionally employed for soft tissue imaging despite its poor ability to precisely render changes in the bone (e.g., micro-calcifications) during initial stages of diseases. The ability to be sensitive to bones and cartilages, and to distinguish the constitutive cells of cartilage, chondrocytes is of tremendous importance. Phase Contrast Imaging (PCI) relies on the property that the X-rays refraction index of materials can be a thousand times greater than the absorption index for light elements. This generates a higher contrast for soft tissues in comparison to the conventional methods based on the sole absorption. Therefore, PCI is able to image all the tissues that constitute the joint having concurrent representation of both high absorbing (e.g., bones) and less absorbing tissues (e.g., fibrous cartilage, ligaments, tendons, meniscus and associated soft tissues (synovial membranes and muscle))<sup>18–21</sup>.

As demonstrated in ref.<sup>20</sup>, X-ray PCI outperforms the other preclinical imaging modalities for

cartilage. The purpose of this protocol is to detail the procedure and to show some representative results. Scheme of the effect of growth factors on immature cartilage explant is shown in **Figure 1**.

## **PROTOCOL:**

All methods described here have been approved by the Ethical Research Committee of Swansea University and biopsy materials were acquired under license from the Department for Environment, Food & Rural Affairs (DEFRA), UK. This protocol follows the animal care guidelines of our institutions.

### **1. Explant Cultures**

#### **1.1. Preparation of the explants from bovine legs scalp**

1.1.1. Prepare absorbent protector and a scalpel, standard surgical scalpel with #10 scalpel blade.

1.1.2. Spray all the materials with 70% ethanol solution.

1.1.3. Soak the bovine leg (7 days-old male bovine steers obtained from the slaughterhouse with veterinary approval) with water to remove all blood and mud.

1.1.4. Clean the leg with soap and scrub with a brush.

1.1.5. When adequately clean, spray the leg with 70% ethanol.

1.1.6. Put it on an absorbent paper.

1.1.7. Cut around the feet with a scalpel.

1.1.8. Trace a delicate line along the length of the leg.

1.1.9. Take extra care in the joint zone.

1.1.10. Remove the skin of the leg carefully along the lengthwise scalpel line.

1.1.11. Put the waste (skin, used tissue, paper and gloves) in a clinical waste bag.

1.1.12. Clean/brush the leg with soap and sterilize with ethanol again when the skin has been removed.

1.1.13. Do not damage the region close to the joint cavity. If the cavity is opened or damaged with blood infiltration, it is not sterile anymore and the leg cannot be used.

221  
222 1.1.14. Place the leg in an Al-foil that have been sprayed with 70% ethanol.

223  
224 1.1.15. Place the appropriately sized latex gloves over the ends of the leg to prevent blood  
225 egress from the proximal end or possible contamination from the hoof.

226  
227 1.1.16. Dispose of the waste materials in the appropriate manner following institutional rules.

## 228 229 1.2. Explant extraction and culture

230  
231 NOTE: The explants must be obtained from the internal part of the joint (**Figure 2**, two first  
232 stages). To be of comparable conditions, four (or six) explants must be punched from the same  
233 zone in order to apply the four (or six) different treatments on samples possessing almost the  
234 same shape and characteristics.

235  
236 1.2.1. Open the laminar flow hood 25 min before use, clean with alcohol 70%.

237  
238 1.2.2. Put the culture medium to warm in a water bath.

239  
240 1.2.3. Prepare a 24 well plate with 1.5 mL of basic medium, DMEM-F12 only (washing medium)  
241 in each well.

242  
243 1.2.4. Prepare another well plate with 1.5 mL of complete culture medium. Store in culture  
244 incubator at 37 °C until use

245  
246 1.2.5. Prepare the material on a rack: one universal tube with 70% ethanol and another  
247 universal tube with washing medium.

248  
249 1.2.6. Prepare a scalpel and a 4 or 6-mm biopsy punch (placed in the alcohol universal tube).

250  
251 1.2.7. Put the tubes and the materials under the hood.

252  
253 1.2.8. Put an absorbent protector sprayed with 70% ethanol under the hood.

254  
255 1.2.9. Prepare some tissues sprayed with 70% ethanol.

256  
257 1.2.10. Take a dissection plate, cover it with Al-foil.

258  
259 1.2.11. Take the same, previously prepared, feet out of the fridge (4 °C) and spray them with 70%  
260 ethanol.

261  
262 1.2.12. Dispose hazardous and clinical bags near the hood to autoclave the waste later.

263  
264 1.2.13. Spray the foot with 70% ethanol.

1.2.14. Move the joint to find the midline of the joint where the incision should be made. Do this under the hood.

1.2.15. Take the sterile scalpel.

1.2.16. Cut carefully along the midline following the contour of the joint edges. Do not touch the metacarpophalangeal joint medial condyle cartilage.

1.2.17. Carefully cut the ligament when the joint is opened.

1.2.18. Throw away the lower part of the feet in an autoclave bag.

1.2.19. Remove all the other tissues in order to expose all the cartilage of the joint (**Figure 2**).

NOTE: Be careful not to touch anything with the feet.

1.2.20. Place the scalpel and biopsy punch in alcohol and then in the washing medium.

1.2.21. Make some circles with this punch (4-5 per face) with some force along the internal faces of the bones.

1.2.22. Place the bio-punch in alcohol when finished to clean it.

1.2.23. Take a scalpel and cut (trace a line) between each circle and along the central line of the bone.

1.2.24. To take out the cartilage explant cut vertically on one of the borders of the circle biopsy, then cut horizontally on the subchondral bone very carefully.

1.2.25. To remove the cartilage explant cut horizontally below the punch line along the subchondral bone and calcified cartilage, the explants will pop out.

NOTE: Explants should have a uniform thickness, if possible.

1.2.26. Place the explant in the well plate filled with 1.5 mL of washing medium.

NOTE: Always perform experimental control and treatment of explants coming from the same location in the joint.

1.2.27. Check that the explant is well orientated correctly. The surface of the explant should be facing up and the subchondral bone part of the explant should face the bottom of the well plate.

1.2.28. Keep the well plate closed in between each biopsy.



309  
310 1.2.29. Remove the washing medium.

311  
312 1.2.30. Wash again with wash medium. Leave in wash medium for 2-3 h. Bone residues, blood  
313 will have time to flux out in the medium.

314  
315 1.2.31. Transfer the explants in a new well plate containing the complete culture medium. Be  
316 careful: don't touch anything with the pipette.

317  
318 1.2.32. Check that explants are still in the right position (bone facing the bottom part of the well-  
319 plate).

320  
321 1.2.33. Clean everything and throw away the clinical waste in adequate place.

322  
323 1.2.34. Once the explants are placed in culture in an incubator at 37 °C with 5% CO<sub>2</sub>, change the  
324 explant culture medium every two days with warm fresh medium to sustain to the diverse needs  
325 of the cells/tissues. Check that explants are still in the right position (bone facing the bottom part  
326 of the well-plate).

## 327 328 1.3. Sample fixation (optional)

329  
330 NOTE: Perform this step after only at the end of the cell culture which means after 3 weeks of  
331 culture. The explants have then reached at matured stage.

332  
333 1.3.1. Wash the explants with DMEM-F12 with a pipette under the tissue culture hood.

334  
335 1.3.2. Wash the explants twice with PBS with a pipette under the tissue culture hood.

336  
337 1.3.3. Fix them overnight at 4 °C by soaking in 10% NBFS (Neutral Buffer Formalin Saline).

338  
339 1.3.4. Place the fixed explants in PBS in a microcentrifuge tube

340  
341 1.3.5. Store the explants at 4 °C. Fixed explants can stay in these conditions up to 6 months.

## 342 343 2. Sample preparation for the imaging session

344  
345 2.1. Use conical plastic tips of an appropriate size (usually 1 mL tip) with the respect to the  
346 sample and the camera field of view.

347  
348 2.2. Seal the cone tip (by heating it with a flame) in order to have a water-proof sample  
349 container.

350  
351 2.3. Fill the tip with PBS. Hold the sample with tweezers and insert it into the tube. Remove  
352 air bubble by slow shakes.

2.4. Mount the tube on the tomography stage and align it by taking simple radiographs.

### 3. X-ray Phase Contrast imaging session

3.1. Place the detector at 2.5 m from the sample

3.2. Set the X-ray photon energy to 17 keV using a double Silicon crystal system within a Bragg-Bragg geometry.

3.3. Mount Imaging detector consisted of a scientific CMOS camera<sup>22</sup> on an optic with a resulting isotropic voxel size of 3.5  $\mu\text{m}$  in the 3D image.

3.4. Use a 60  $\mu\text{m}$  thick Gadolinium Oxysulfide scintillator screen to convert the X-ray to visible light

3.5. Data collection: Acquire 2000 projections during a 360° scan of the sample with an exposure time of 2 s for each projection.

3.6. Use a the phase retrieval algorithm to extract the phase signal as described in ref.<sup>23</sup>. The algorithm uses an a priori knowledge of the complex refractive index distribution within the sample. The main hypothesis, not verified here, is that there is one material to reconstruct. In this particular case, the ratio between the refraction and the absorption index set to 1,200 which was experimentally observed to the best compromise for bone and cartilage visualization.

3.7. Use the standard filtered back projection CT reconstruction algorithm using an open-source, Graphics Processing Unit (GPU)-based implementation of the PyHST2 code<sup>24</sup>.

### REPRESENTATIVE RESULTS:

A simple propagation based imaging set-up was used<sup>25</sup> as sketched in **Figure 3**. In synchrotron propagation-based imaging, a coherent X-ray beam illuminates the object, giving rise to spatially varying phase shifts<sup>19</sup>. As the X-ray beam propagates after the sample, the distorted wave front generates characteristics pattern. By analyzing these characteristic patterns with dedicated algorithms<sup>23</sup>, the phase shifts caused by the sample is numerically retrieved.

Representative phase contrast imaging slices using the described methodology are shown in **Figures 4** and **Figure 5**.

After the 3 weeks of culture, explants were fixed as previously described. Once fixated, explants can be kept at 4 °C up to 6 months. This experiment has been performed approximately 30 days after their fixations. **Figure 4** is a 3.5  $\mu\text{m}$  thick axial plane section within the cartilage part of the sample. Therein, one clearly sees the chondrocytes (thin black round structures), some specific chondrocyte cells transforming into osteocytes (smaller white round structures), as well as variations in the density of the extracellular cartilage matrix. Moreover, one can distinguish

sparse bigger tubular structures that are the vascular canals supporting the bone formation. Some ring artefacts can be seen especially in the center of the image. The ring artefacts are caused by pixel-dependent response of the detector that can be solved either by using advanced image processing techniques<sup>26</sup> or with a longer acquisition time that increase the signal to noise ratio. For the present study this artefact did not affect the extracellular matrix analysis.

**Figure 5** shows sagittal plane sections with different gray level windows to highlight the capability of phase contrast imaging to render all the different tissues. In **Figure 5A**, grey values were chosen for bone visualization while in panels **Figure 5B,C**, grey values were set for the cartilage representation. The panel C is a zoom inset of panel B centered on a wound made during the biopsy. In these images, one can observe the trabecular structure of the subchondral bone (panel A). In the cartilage part (**Figure 5B**), the yellow arrows indicate the vascular canals. As expected, the size of chondrocytes decreased from the bone plate down to the superficial zone of the cartilage. The centered part of the cartilage plug presented a necrosis (reduction of the matrix density). Some variation in density within the cartilage extra cellular matrix were also observed. It is interesting to note that 21 days after the wound, cells actively working for the repair of this fracture were observed (**Figure 5C**). Additionally, a hypersignal of the extra cellular matrix was revealed around the fracture, corresponding to a high density.

**Figure 6** shows axial and sagittal planes of two samples conditions (Condition 1 : ITS control, without any growth factors added to the culture medium and condition 2: ITS FT-treated, growth factors were present in culture medium, see protocol for details). The images were scaled with the same grey level window for highlighting the changes in the cartilage matrices. The control sample is on the left column and the sample treated with growth factors is shown in the right. In these images it is clear that the growth factor induced changes in the cartilage extra cellular matrix than the control one. The canals in the control sample were empty while one can see dense material within the treated samples canals. Close to bone structures some cells in specification were visible only in the growth factor treated cartilage.

#### FIGURE AND TABLE LEGENDS:

**Figure 1: Scheme of growth factors effects on immature cartilage explants (A).** FGF-2 and TGF- $\beta$ 1 induce maturation-like changes that lead to an identical biophysical profile to mature cartilage including water content, collagen and proteoglycan content and biomechanical properties. In addition there was significant resorption from the base of the explant leading to a reduction in height<sup>2</sup>. Grey spheres are the chondrocytes and pinkish curved lines are the collagen fibrils. This sketch is a summary from reference<sup>2</sup>. At an immature state, chondrocytes and collagen fibrils were randomly distributed within the tissue. At a mature stage, the chondrocytes were distributed along the arcadian structure-like collagen fibrils with different size and morphology (as well described in the literature). Polarized light microscopy of picro-sirius red stained sections (**B,C**) showed significant changes in collagen organization including denser and more collagen fibrils aligned perpendicularly to the surface but these changes were confined to pericellular regions. Maturation induced by FGF-2 and TGF- $\beta$ 1 (**C**) appeared to be an intermediate state of change compared to the final phase where the collagen fibril orientation is perpendicular to the

surface in the mid/deep layers of cartilage. For more details and information about this biological model, please read articles<sup>2,3,14–16</sup>.

**Figure 2: Flowchart of the experimental procedure from explant culture to analyses.** 6 mm-diameter biopsies of bovine articular cartilage (AC) from the metacarpophalangeal joint on the left. Here, an opened joint under sterile conditions of immature AC (7-days old steer) is shown. In the insert, some biopsies showed some cartilage facing up, some other biopsies cartilages facing down. Immature explants biopsies present a white shining part corresponding to the cartilage and another pinkish part corresponding to calcified cartilage and subchondral bone). In the middle, the explants were placed in culture for 3 weeks with the appropriate treatments. Then, they undergo diverse analyses. Some examples are shown in the right of the figure.

**Table 1: Selenium Medium Reagents**

**Figure 3: X-ray Phase Contrast Propagation Based Imaging Set-up.**

**Figure 4: Thin axial slice of phase contrast imaging of the treated cartilage explant.** Noteworthy structures and cell types are indicated by yellow arrows.

**Figure 5: Sagittal thin slice of phase contrast imaging of maturing cartilage.** (A) Bone window (B) cartilage window (C) inset in the cartilage matrix centered on a fracture.

**Figure 6: Comparison of Phase Contrast imaging of two samples.** Control explant (A and C) and explant cultured with growth factor treatment (B and D). Axial slices (A and B) and sagittal slices (C and D).

## DISCUSSION:

We presented a complete study from the sample preparation to the image visualization, including the data acquisition protocols, for the study of in-vitro fast maturing articular cartilage. Results of a synchrotron imaging session showed the goodness of the model.

In the model presented here, some observations and limits must be mentioned. This “accelerated maturation” occurs within 21 days of culture. For longer culture periods, explant plugs begin to degrade with change in cellular metabolism and cartilage ECM components (i.e., collagens and proteoglycans) contents as detailed in ref.<sup>27</sup>. Still, in our model, within the limit of 21 days, the tissue remains stable<sup>2,3</sup>. The complex remodeling dynamics of the model can be assessed. While the matured cartilage is mimicking an adult cartilage with respect to biochemical and biomechanical properties, the presented model does not display the full reorganization of collagen orientation similar to that seen in mature cartilage. We believe this is due to the overexpression of lysyl oxidase-L1 (LOXL1) isoform which induces crosslinking within the tissue and therefore inhibiting any further collagen reorganization<sup>10</sup>. The mechanics of cartilage growth have been modeled by a continuum mixture model<sup>28</sup>. The static environment with a lack of mechanical stimuli in which our samples were cultured can then be another potential explanation. This represent an important parameter that should be investigated for AC exposed

to a selenium deficient environment.

The sample preparation must be carried out in sterile conditions, each being important for the sample conditioning. The sample fixation is however not mandatory for the imaging session. Without fixation, samples must be directly imaged after the three weeks of culture. This model is suited to be used in three weeks culture sessions. No delay can then be accepted because at the end of the culture, other inconveniences can appear such as slight necrosis in the central core of the explants. The sample being not fixed, it must be handled carefully to limit biological degradation. It can be used for other experiments such as PCR, ICP-MS, and histology for example. However, in our case, the samples were chemically fixed for the sake of testing different imaging modality (not presented here) on the same explants. Synchrotron beamtimes present restricted accesses. Samples must be then ready to analyze for better conveniences. The main difficulty encountered in the sample preparation is the explant culture, the joint having to be opened under a sterile hood to avoid any bacterial contamination. During the biopsy, the explant must also be rinsed several times before being placed in culture to remove all blood cells that may induce contamination. The fast maturing protocol employed here permitted to generate valid samples within days and presenting biologically relevant features. The variability of the sample diameters is explained by the best compromise with joint size and having a sample size that can be statically relevant. Below 4 mm we don't have enough matter to sustain an explant culture and more than 6mm the punch is larger than the joint size. This does not impact the imaging session as the image field of view at this resolution can be up to 14 x 14 mm<sup>2</sup> in the reconstruction plane. The height of the sample is not a limitation either because we can stack several acquisitions. For X-ray PCI, the quality of the reconstructions may be affected by important parameters. X-ray Phase contrast Imaging is highly sensitive to air bubbles that can be forming in the surrounding liquid environment where the sample is resting. For a good reconstruction, a minimum number of slices with both cartilage and bone are necessary. For this reason, we place the sample with the bone plate parallel to the beam propagation plane.

The main goal of this experiment was to study whether X-ray PCI is a suitable imaging candidate for following-up the cartilage maturation process. Histological techniques would probably have a better specificity, but they are destructive and strictly limited to 2D investigation while the employed technique here is fast and non-invasive. The imaging procedure presented here is rather simple with the numerical processing of the data. The main drawback of the technique is the required large transverse coherence and the beam collimation, available solely at synchrotrons or sophisticated x-ray sources. Nevertheless, the access to synchrotron imaging beamlines is feasible all over the world with public proposal acceptance. The choice of the energy is critical. Depending on the energy chosen the bone can induce metal-like artefacts. In this study, we chose an energy of 17 keV at which bone can cause strong artefacts whilst we have a very good contrast in the cartilage matrix. Raising up the energy would solve the bone artefacts whilst decreasing the image quality of the cartilage matrix. As the cartilage was the main choice, we had to make this compromise. Due to this employed imaging protocol we could reveal in 3D some subtle changes in the extracellular matrix as well as cell morphology that cannot be visualized with other modalities. The results demonstrate that X-ray Phase Contrast Imaging (PCI) can render, within a single acquisition, bone and cartilage tissues in a relatively fast acquisition time

(approximately 1 h). Moreover, both cells types (chondrocytes and osteocytes) are visible simultaneously, as well as variations within the cartilage extracellular matrix. This protocol and the typical obtained results open the possibility to have better comprehensive studies of the cartilage mechanics and biology. One can assume that this method can be applied dynamically to scrutinize the behavior of chondrocytes within the joints. The perspectives of the 3D macro and microscopic investigation of joints in situ and in vivo are highly exciting and seems feasible thanks to developments in X-ray sources and X-ray phase contrast imaging<sup>29,30</sup>. Ultimately, this would allow to explore the chondrocytes function under loading conditions that remains a mystery. Further studies will be carried out to exploit these new PCI capabilities on a large sample database following the same preparation protocol.

#### ACKNOWLEDGMENTS:

Authors thank the ESRF for providing in house beamtime. Authors would like to thank Eric Ziegler for scientific discussions. The described PCI experiment was conducted at the beamline BM05 of the European Synchrotron Radiation Facility (ESRF), Grenoble, France. CB thanks Explora'doc Auvergne Rhone Alpes and scholarships from the University of Swansea and the Université Grenoble Alpes for funding part of this study.

#### DISCLOSURES:

None

#### REFERENCES:

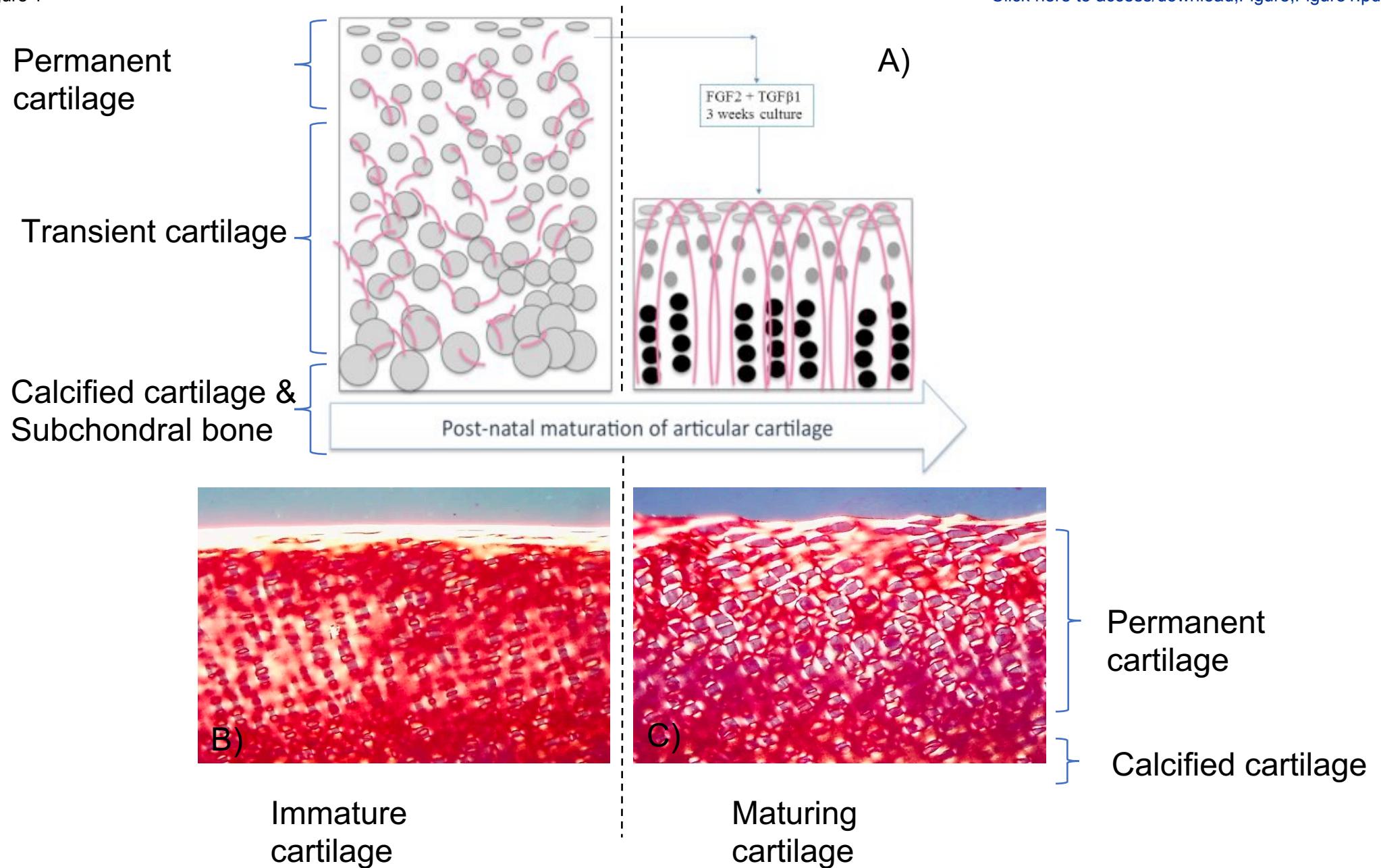
1. Little C. B., Ghosh P. Variation in proteoglycan metabolism by articular chondrocytes in different joint regions is determined by post-natal mechanical loading. *Osteoarthritis and Cartilage*. **5** (1), 49-62 (1997).
2. Khan I. M. et al. Fibroblast growth factor 2 and transforming growth factor  $\beta$ 1 induce precocious maturation of articular cartilage. *Arthritis and Rheumatology*. **63** (11), 3417-3427 (2011).
3. Khan I. M. et al. In vitro growth factor-induced bio engineering of mature articular cartilage. *Biomaterials*. **34** (5), 1478-1487 (2013).
4. Ascorbate. <http://www.sigmaaldrich.com/life-science/cell-culture/learning-center/media-expert/ascorbate.html>
5. McNulty, A. L., Vail, T. P., Kraus, V. B. Chondrocyte transport and concentration of ascorbic acid is mediated by SVCT2. *Biochimica et Biophysica Acta - Biomembrane*. **1712** (2), 212-221 (2005).
6. Clark, A. G., Rohrbaugh, A. L., Otterness, I., Kraus, V. B. The effects of ascorbic acid on cartilage metabolism in guinea pig articular cartilage explants. *Matrix Biology*. **21** (2), 175-184 (2002).
7. Transferrin. <http://www.sigmaaldrich.com/life-science/cell-culture/learning-center/media-expert/transferrin.html>
8. Liu, X. et al. Role of insulin-transferrin-selenium in auricular chondrocyte proliferation and engineered cartilage formation in Vitro. *International Journal of Molecular Sciences*. **15** (1), 1525-1537 (2014).

9. French, M. M., Athanasiou, K. A. Differentiation Factors and Articular Cartilage Regeneration. In *Topics in Tissue Engineering*. Eds. Ashammakhi, N., Ferretti, P. (2003).
10. Zhang, Y. et al. Platelet-rich plasma induces post-natal maturation of immature articular cartilage and correlates with LOXL1 activation. *Science Reports*. **7** (1), e3699 (2017)
11. Schepman, K., Engelbert, R. H. H., Visser, M. M., Yu, C., De Vos, R. Kashin Beck Disease: More than just osteoarthritis - A cross-sectional study regarding the influence of body function-structures and activities on level of participation. *International Orthopedics*. **35** (5), 767-776 (2011).
12. Sudre P, Mathieu F. Kashin-Beck disease: From etiology to prevention or from prevention to etiology? *International Orthopedics*. **25** (3), 175-179 (2001).
13. Allander, E. Kashin-Beck Disease. An analysis of Research and public health activities based on a bibliography 1849-1992. *Scandinavian Journal of Rheumatology*. **23** (S99), 1-36 (1994).
14. Bissardon, C. et al. Sub-ppm level high energy resolution fluorescence detected X-ray absorption spectroscopy of selenium in articular cartilage. *Analyst*. **144** (11), c9an00207c (2019).
15. Bissardon C. *Role of Selenium in Articular Cartilage Metabolism, Growth and Maturation*. University of Swansea (Swansea (GB)); 2016. Accessed May 25, 2020. <https://tel.archives-ouvertes.fr/tel-01942169>.
16. Bissardon, C., Charlet, L., Bohic, S., Khan I. Role of the selenium in articular cartilage metabolism, growth, and maturation. In: *Global Advances in Selenium Research from Theory to Application - Proceedings of the 4th International Conference on Selenium in the Environment and Human Health, 2015*. (2016).
17. Winkel, L. H. E. et al. Environmental selenium research: From microscopic processes to global understanding. *Environment Science Technology*. **46** (2), 571-579 (2012).
18. Bravin, A., Coan, P., Suortti, P. X-ray phase-contrast imaging: From pre-clinical applications towards clinics. *Physics in Medicine and Biology*. **87** (1034), 20130606 (2014).
19. Horng, A. et al. Cartilage and soft tissue imaging using X-rays: Propagation-based phase-contrast computed tomography of the Human Knee in comparison with clinical imaging techniques and histology. *Investigative Radiology*. **49** (9), 627-634 (2014).
20. Labriet, H. et al. High-Resolution X-Ray Phase Contrast Imaging of Maturing Cartilage. *Microscopy and Microanalysis*. **24** (S2), 382-383 (2018).
21. Rougé-Labriet, H. et al. X-ray Phase Contrast osteo-articular imaging: a pilot study on cadaveric human hands. *Science Reports*. **10** (1911), s41598 (2020).
22. Mittone, A. et al. Characterization of a sCMOS-based high-resolution imaging system. *Journal of Synchrotron Radiation*. **24** (6), 1226-1236 (2017).
23. Paganin, D., Mayo, S. C., Gureyev, T. E., Miller, P. R., Wilkins, S. W. Simultaneous phase and amplitude extraction from a single defocused image of a homogeneous object. *Journal of Microscopy*. **206** (1), 33-40 (2002).
24. Mirone, A., Brun, E., Gouillart, E., Tafforeau, P., Kieffer, J. The PyHST2 hybrid distributed code for high speed tomographic reconstruction with iterative reconstruction and a priori knowledge capabilities. *Nuclear Instruments and Methods in Physics Research Section B: Beam Interactions with Materials and Atoms*. **324**, 41-48 (2014).
25. Bravin, A., Coan, P., Suortti, P. X-ray phase-contrast imaging: from pre-clinical applications towards clinics. *Physics in Medicine and Biology*. **58** (1), R1-R35 (2013).

- 617 26. Vo, N. T., Atwood, R. C., Drakopoulos, M. Superior techniques for eliminating ring artifacts  
618 in X-ray micro-tomography. *Optic Express*. **26** (22), 28396 (2018).
- 619 27. Moo, E. K., Osman, N. A. A., Pingguan-Murphy, B. The metabolic dynamics of cartilage  
620 explants over a long-term culture period. *Clinics*. **66** (8), 1431-1436 (2011).
- 621 28. Stender, M. E. et al. Integrating qPLM and biomechanical test data with an anisotropic  
622 fiber distribution model and predictions of TGF- $\beta$ 1 and IGF-1 regulation of articular cartilage fiber  
623 modulus. *Biomechanics and Modeling in Mechanobiology*. **12** (6), 1073-1088 (2013).
- 624 29. Labriet, H. et al. 3D histopathology speckle phase contrast imaging: from synchrotron to  
625 conventional sources. In: *Medical Imaging 2019: Physics of Medical Imaging*. Eds. Bosmans, H.,  
626 Chen, G-H., Gilat Schmidt, T. 10948, SPIE 63 (2019).
- 627 30. Zdora, M. C. et al. X-ray Phase-Contrast Imaging and Metrology through Unified  
628 Modulated Pattern Analysis. *Physics Review Letters*. **118** (20), 203903 (2017).
- 629



Figure 1



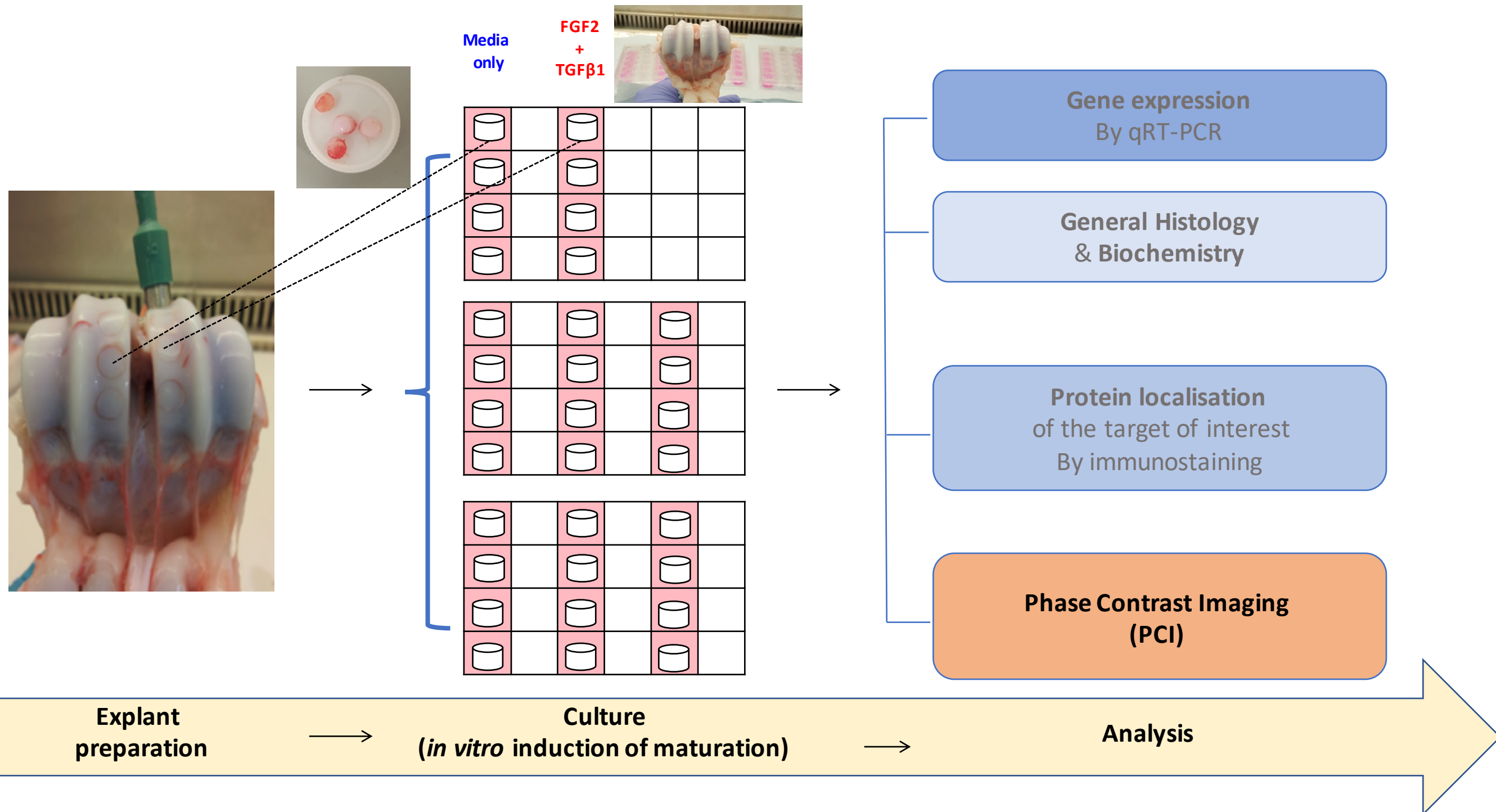
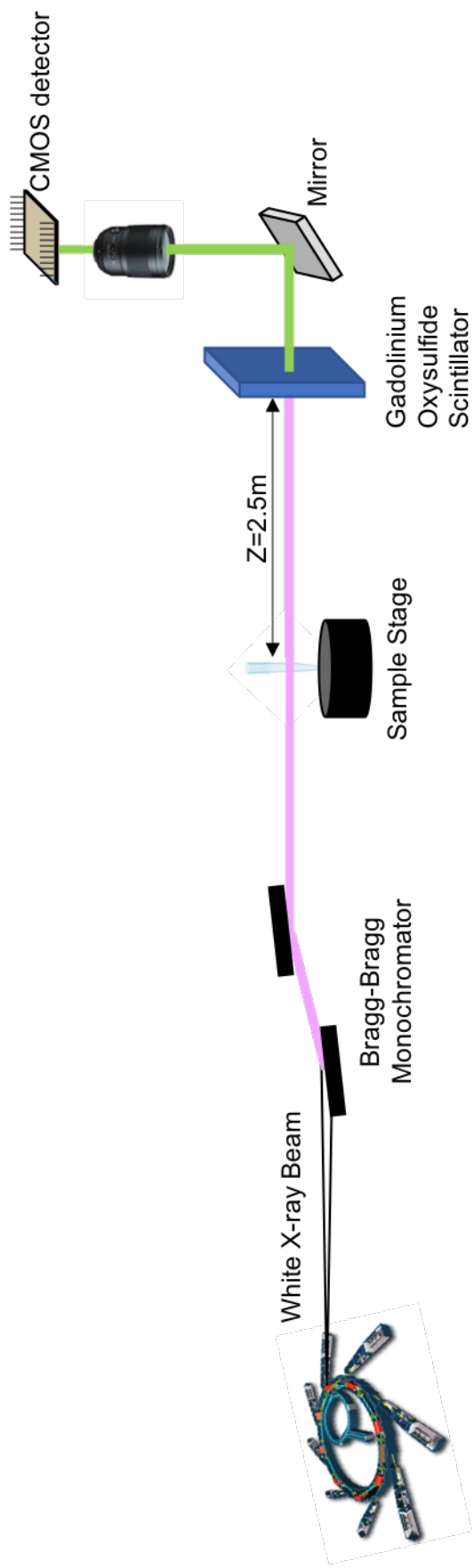


Figure 3



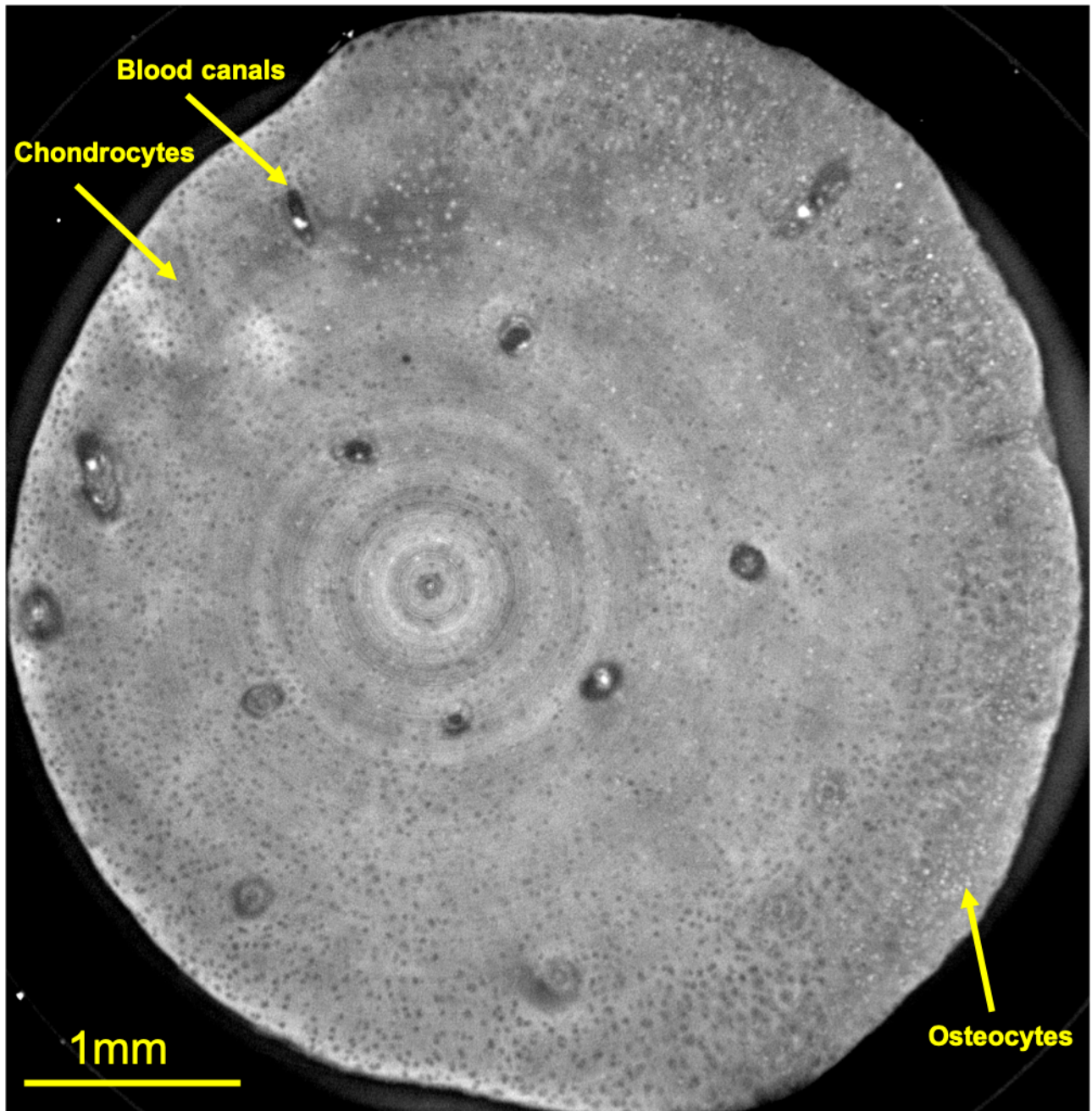
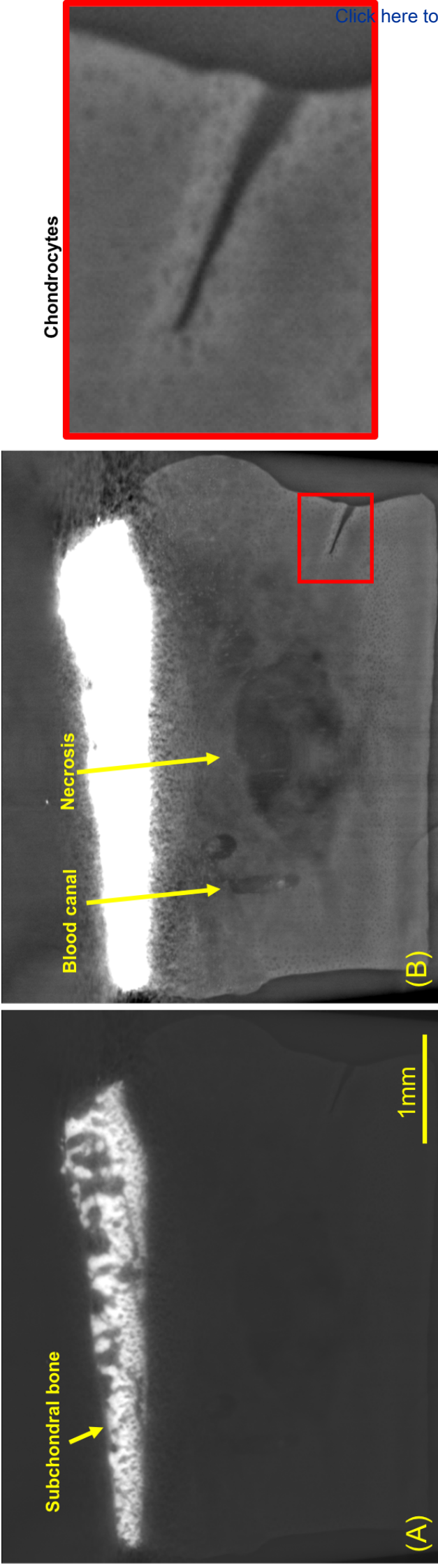
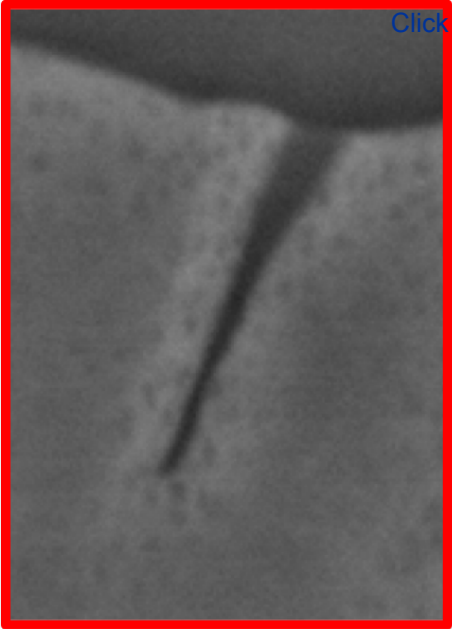


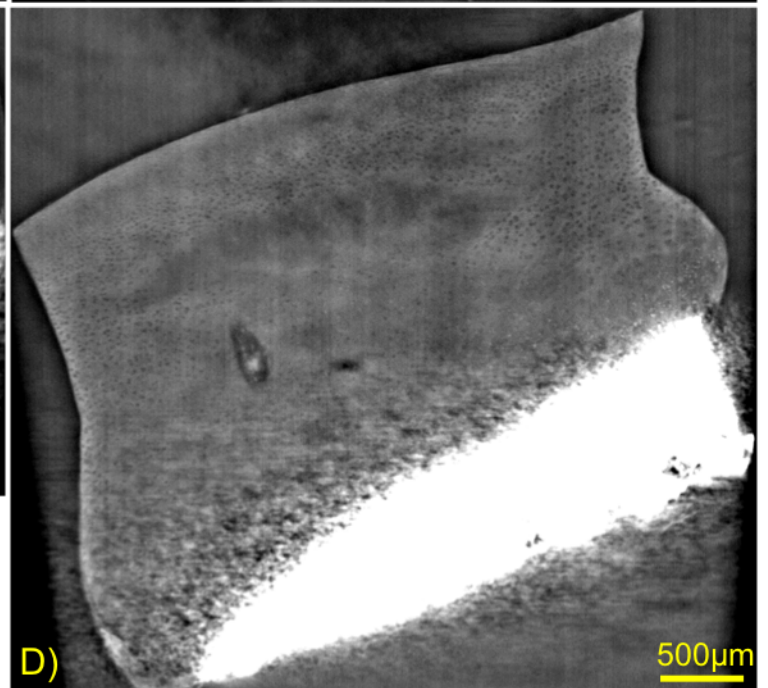
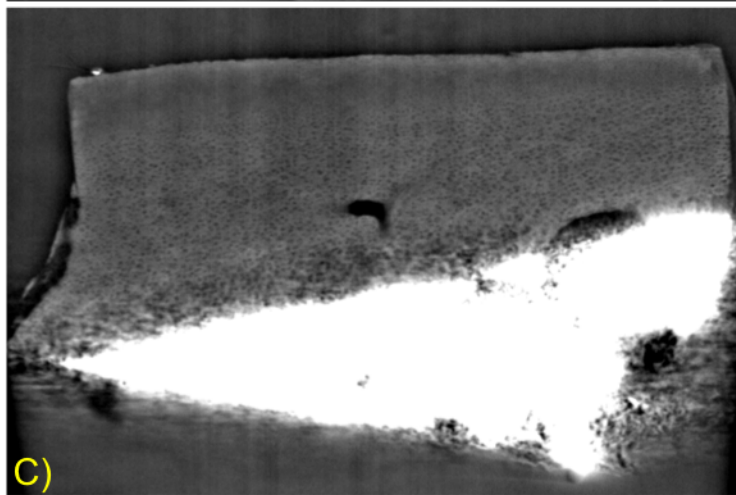
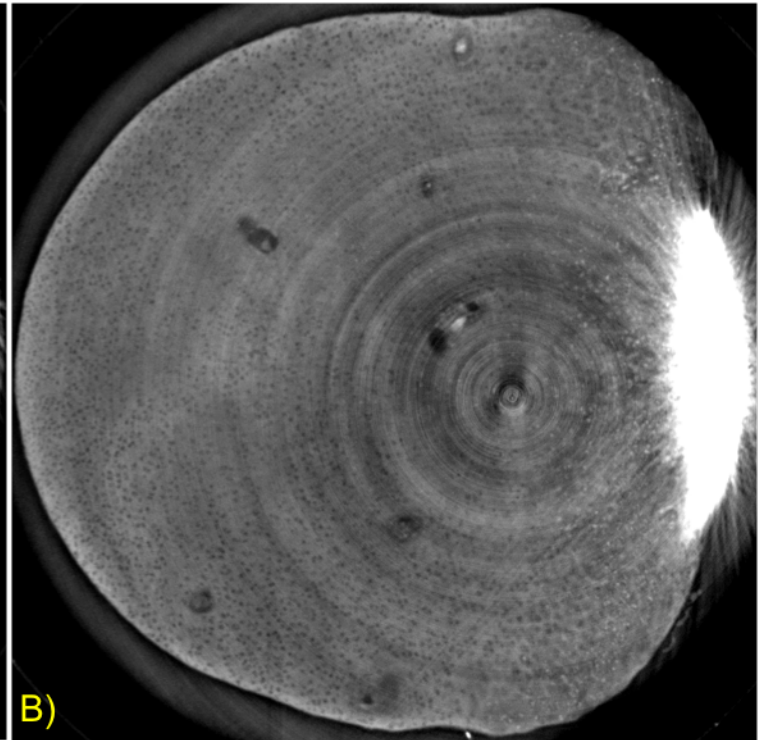
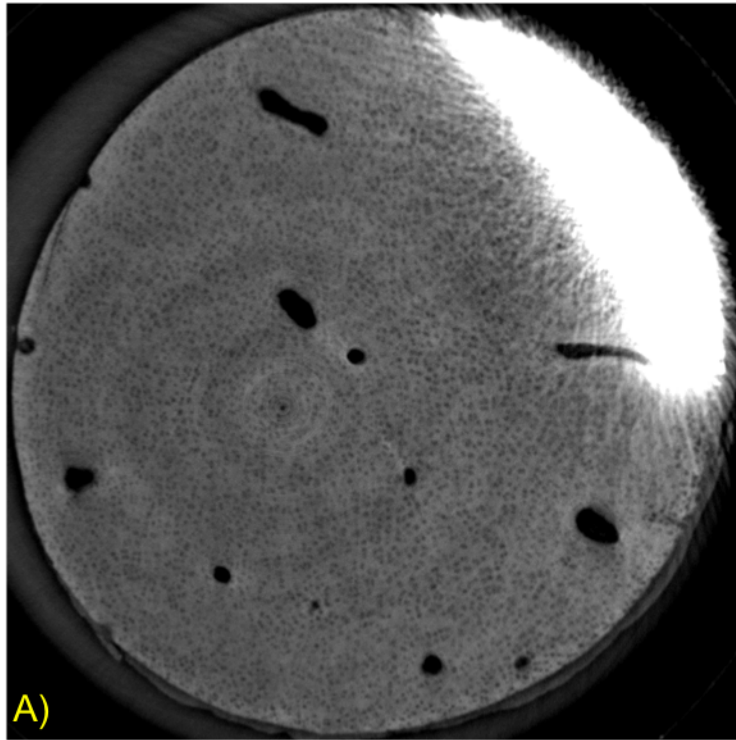


Figure5



Chondrocytes





Reagents	Quantities
DMEM F12	440 mL
Ascorbic acid	50 mg
Gentamicin	500 µL
HEPES	5 mL
ITS	5 mL

<b>Name of Material/ Equipment</b>	<b>Company</b>
<b>Material : Biological products</b>	
DMEM/F-12 (1:1) (1X) + GlutaMAX Dulbecco's Modified Eagle Medium	
F-12 Nutriment Mixture (Ham) 500mL	Gibco by life technologies
Gentamicin Reagent Solution, 50 mg/mL	Gibco by life technologies
HEPES, special preparation, 1M, pH 7.5 filtered	Sigma
ITS, Insulin-Transferrin-Selenium	Gibco by life technologies
L-Ascorbic Acid-2-Phosphate, sesquimagnesium salt hydrate, 95%	Sigma
Neutral Buffer Formalin (NBF)	Sigma Aldrich
phosphate buffered saline (PBS) pH 7.4	Gibco by life technologies
<b>Culture equipments:</b>	
Absorbent Protector, Benchkote	WhatmanTM
Accurpette VWR	
Autoclavable Disposal Bag	
biopsy punches	MILTEX by KAI
Clinical waste for alternative treatment Medium Duty	
Eppendorf tubes	
Falcon tubes	
free of detectable RNase, DNase, DNA&Pyrogens 1000ul Bevelled	
Graduated, filter tip	Starlab, TipOne (sterile)
free of detectable RNase, DNase, DNA&Pyrogens 20µl Bevelled	
Graduated, filter tip	Starlab, TipOne (sterile)
free of detectable RNase, DNase, DNA&Pyrogens 200ul Bevelled	
Graduated, filter tip	Starlab, TipOne (sterile)
Incubator	
Optical microscope	



Pipette-boy

Pipettes (25-10-5 ml)

Plastic tweezers

Scalpel

Tips

Tissue culture hood

Vacuum pump

Water bath 37°C

well plates

**Protection equipment:**

face shield

gloves

lab coat

safety goggles

**Data acquisition equipment:**

Fiji software

PyHST reconstruction toolkit

Synchrotron Radiation Facility (monochromatic X-ray beam)

CellStar, Greiner Bio-one

Oxford Instrument

Catalog Number	Comments/Description
31331-028	
15750-060	
H-3375	
51500-057	
A8960-5G	
HT501128	
10010023	
Cat No. 2300731,	Polysterene Backed, 460cm*50m
ref 33-36	<p>For disposal of contaminated plastic laboratory ware neck should be left open to allow penetration of steam, Hazardous Waste, STERILIN (white bag)</p> <p>4 &amp; 6 mm diameter</p> <p>(UN-approved weight 5kg, Un-closure methods, UN- SH4/Y5/S/II/GB/4/06 (orange bag)</p> <p>0.5mL and 1.5 mL</p> <p>15mL and 50 mL</p>
S1122-1830	
S1120-1810	
S1110-1810	Incubator at 37°C, humidified atmosphere with 5% CO2

25mL-, 10mL-, and 5mL sterile plastic-pipettes

AGT 5230

P1000, P200 and P10 with P1000, P200 and P10  
tips (sterile)

12 & 24 well plates

open source Software  
open source Software

Dear Editorial board,

We thank you and the reviewers for the time spent reviewing our manuscript. We believe the reviewers' comments have led to an improvement of our manuscript. Enclosed to the submission you'll find a track version of the word document to see the changes together with the final version. Below is the point by point response to the last comments.

## Editorial comments:

**1. The editor has formatted the manuscript to match the journal's style. Please retain and use the attached version for revision.**

Ok

**2. Please address all the specific comments marked in the manuscript.**

Done

**3. For the question on the submission website, Please confirm that you have read and agree to the terms and conditions of the author license agreement that applies below: Please select I agree to UK Author License Agreement. This is important.**

We will try to do this ;)

**4. Please also check with your funding source that you are allowed to publish a standard access article. Also please confirm that you will be able to deposit the article to PMC on your own if required.**

Checked. What is PMC? If it is pubmed central we confirm that we will be able to deposit the article

**5. The manuscript needs thorough proofreading.**

We hope to receive real proofs and not a word document for proofreading As the word document can vary in length on Windows or AppleOS I do not trust this document for checking this out. Please provide us a real proof in pdf to check

**6. Once done please ensure that the highlight is no more than 2.75 pages and no less than 1 page including headings and spacings.**

Same remark concerning the proof

**7. Please reformat the figure legends. Each Figure Legend should include a title and a short description of the data presented in the Figure and relevant symbols. The Discussion of the Figures should be placed in the Representative Results.**

We put a title and changed the letters in capital.

**8. Please reword lines: 44-47, 54-55, 83-87, 154-169 as it matches with previously published literature.**

Done

**9. If any of the figures are reused: Please obtain explicit copyright permission to reuse any figures from a previous publication. Explicit permission can be expressed in the form of a letter from the editor or a link to the editorial policy that allows re-prints. Please upload this information as a .doc or .docx file to your Editorial Manager account. The Figure must be cited appropriately in the Figure Legend, i.e. "This figure has been modified from [citation]."**

No figures were reused